International Journal of Control and Automation
Vol. 8, No. 2 (2015), pp. 153-162
http://dx.doi.org/10.14257/ijca.2015.8.2.16

Modeling and Dynamic Analysis of Planetary Gear Transmission Joints with Backlash

Shiwen He*, Qingxuan Jia, Gang Chen and Hanxu Sun

School of Automation, Beijing University of Posts and Telecommunications, 400065 China
**Corresponding Author: Shiwen He. E-mail:bupthsw@gmail.com*

Abstract

As one of the core components, the joint plays an important role during the movement of space manipulator, and its performance will be influenced by the existence of the backlash, which can severely sacrifice the quality of the manipulator to perform a task. In order to have a comprehensive understanding of the influence of the backlash to the gear transmission joints, a dynamic model of planetary gear transmission joint with consideration of the time-varying mesh stiffness, mesh damping, gear backlash, and gear mesh error is established by the lumped parameter method, and the differential equations of motion are established by Newton-Euler method in this paper. In addition, a novel calculation method is proposed to solve the differential equation analytically using the precise integration algorithm under Hamiltonian system on the basis of a simplified treatment. The simulation results indicate that the backlash within a certain range has little effect on periodic solutions of the planetary gear transmission train, but with the enlargement of backlash, the dynamic response of the system is significantly changed.

Keywords: *planetary gear, backlash, nonlinear dynamics*

1. Introduction

Planetary gear transmission joint is widely used in large space manipulators because of its large bearing capacity, high reliability, and long life-span [1]. However, backlash, regarded as one of the most important nonlinearities, may cause delays, oscillations and inaccuracy, leading to the poor performance of control systems in many applications [2-4].Therefore, with the increasing requirements in manipulators performance and control accuracy, dynamic performance of gear pair has been a popular topic in academic research in recent years. Among these, dynamic modeling and performance analysis of the planetary gear transmission with backlash have attracted much attention.

For example, Z. M. Sun [5] established nonlinear dynamic model of planetary gear transmission in consideration of the backlash and mesh stiffness. M. Hamed [6] presented a mathematical model based on dynamic transmission error to analyze the influence of nonlinear oscillations of spur gear pairs with backlash on planetary gear pairs. Q. L. Huang [7] set an optimized mathematical model of gear transmission system on the basis of a nonlinear purely rotational dynamic model of a multistage closed-form planetary gear, aiming at minimizing the vibration displacement of the low-speed carrier. Y. F. Chen [8] investigated the influence of the rotary inertia of the sun gear on the dynamic behavior using a lumped-parameter model of a single-stage planetary gear train. G. Yi [9] studied the correlation between nonlinear tooth wedging and planet bearing forces by analyzing the dynamic response of planetary gear, in which tooth separation, back-side contact, tooth wedging and bearing clearances were taken into account. S. Tao [10] established a lateral-torsion coupled model with multiple clearances to analyze the nonlinear dynamics of a planetary gear system, in which the solutions were determined by harmonic balance method. J.W. LU [11] adopted lumped mass method to build a dynamic

ISSN: 2005-4297 IJCA

model of planetary gear reducer, in which backlash and time-varying mesh stiffness were included, and the solution was carried out using Adams variable step size multistep integration algorithm.

All the research presented above show that the dynamic models of planetary gear transmission system are established based on the Lagrange dynamics through force balance relationship among each stage gear pair, which is especially at a disadvantage to solve the model with large numbers of equations and variables. In addition, the nonlinear backlash is taken into account directly in the process of establishing the dynamic model, which is bad for calculation due to the repeated call of backlash. As a result, a novel modeling method which can accurately establish dynamic model of planetary gear transmission and improve the calculation efficiency is proposed in the paper on the basis of an approximate treatment to the nonlinear backlash and a dimensionless processing to the dynamic model. The paper is arranged as follows: Section 2 establishes an elaborate dynamic model. A novel processing method in Hamiltonian system is proposed in Section 3. Section 4 carries out simulation to verify the method. Conclusions are given in Section 5.

2. Dynamic Model of Joint with Planetary Gear Reducer

2.1. The Mathematical Model of Planetary Gear Reducer

A joint with planetary gear reducer is shown in Figure 1. The actuator motor turns the load through a 2K-H planetary gear reducer. A planetary gear dynamic model is consist of the sun gear (subscripts s), the planet gear (subscripts pi, $i=1,2\cdots n$), the ring gear and carrier (subscripts c), where each stage has n planet gears as shown in Figure 2.

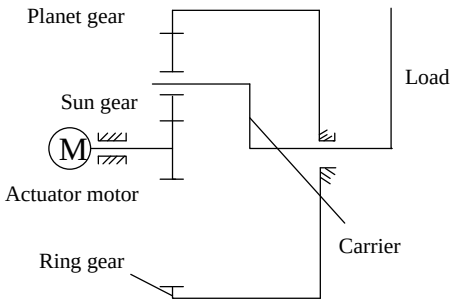

Figure 1. Joint with Planetary Gear Reducer

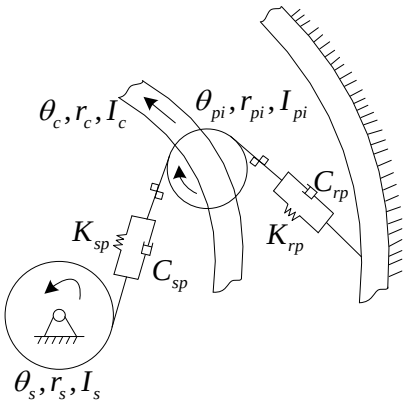

Figure 2. Planetary Gear Dynamic Model

The nonlinear model is established by the lumped parameter method in the following hypotheses:

(1) All the planetary gears are assumed to be spur gears with the same physical and geometrical parameters.

(2) The influence of friction in the process of the gear mesh can be neglected.

Each corresponding mathematical model (Figure 1) is obtained by Newton-Euler method as follows:

The analysis of the sun gear:

$$J_s\ddot{\theta}_s = T_D - \sum_{i=1}^{n}[P_{spi} + D_{spi}] \cdot r_s \tag{1}$$

The analysis of the *ith* planet gear:

$$J_{pi}\ddot{\theta}_{pi} = \left(P_{spi} + D_{spi} - P_{rpi} - D_{rpi}\right) \cdot r_{pi} \tag{2}$$

The analysis of the carrier:

$$(J_c + \sum_{i=1}^{n} m_{pi} r_c^2)\ddot{\theta}_c = \sum_{i=1}^{n}\left(P_{spi} + D_{spi} + P_{rpi} + D_{rpi}\right) \cdot r_c \cdot \cos(\alpha) - T_L \tag{3}$$

Where, J (subscripts s, pi, c) is the inertia ranged from sun gear to planet carrier, r_s is the base circle radius, r_c is the carrier radius which is equivalent to the pitch circle radius of sun gear add to the pitch circle radius of planet, m (subscript pi) is mass of planet gear, α is the mesh angle of gears, T_D is the input matrix, T_L is the load matrix, and P, D (subscripts spi, rpi) are elastic mesh force and viscous mesh force, in which subscript spi represents the internal meshing between sun gear and the planet gear and subscript rpi represents the external meshing between the planet gear and carrier, respectively.

With the symbol δ is used to represent the relative displacement in the direction of the meshing line, the relative displacement between the sun gear and the planetary gear and the relative displacement between the planetary gear and the carrier are respectively written as follows:

$$\begin{cases} \delta_{spi} = \theta_s r_{bs} - \theta_{pi} r_{bpi} - \theta_c r_c \cos\alpha - e_{spi}(t) \\ \delta_{rpi} = \theta_{pi} r_{bpi} - \theta_c r_c \cos\alpha - e_{rpi}(t) \end{cases} \tag{4}$$

Where, e is the composite error function in the process of gear meshing. The elastic mesh force and viscous mesh force of the parts can be written as follows:

$$\begin{cases} P_{spi} = K_{spi}(t) f(\delta_{spi}, b_{spi}) \\ D_{spi} = C_{spi}\dot{\delta}_{spi} \end{cases} \tag{5}$$

$$\begin{cases} P_{rpi} = K_{rpi}(t) f(\delta_{rpi}, b_{rpi}) \\ D_{rpi} = C_{rpi}\dot{\delta}_{rpi} \end{cases} \tag{6}$$

Where, $2b$ (subscripts spi, rpi) represents the backlash which is changed from internal meshing gear set to external meshing gear set. $K(t)$ (subscripts spi, rpi) is time-varying mesh stiffness along the action line, t is the time, C (subscripts spi, rpi) is the damping coefficient of the gear set meshing which is taken as constant, and f is the nonlinear backlash function. The computation of the above parameters will be describes in the following section in detail.

2.2. The Computation of Model Parameters

The transformation law of time-varying mesh stiffness is taken as rectangular wave according to mesh stiffness characteristics of spur gear [12]. The specific transformation law with the relevant parameters is shown in Figure 3. Where, T is the mesh cycle,

$K_{\max}$ and $K_{\min}$ can be defined as the maximum value and minimum value of the mesh stiffness, respectively. φ_0 is the initial phase during the meshing.

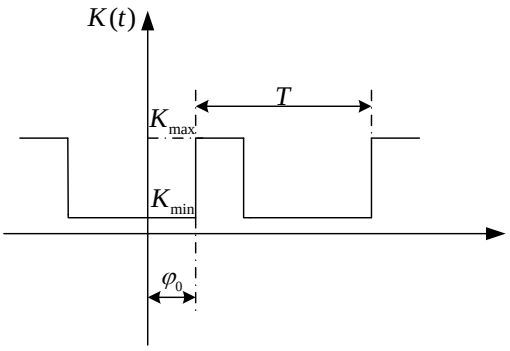

Figure 3. The Time-varying Mesh Stiffness

Taking the mesh frequency as the baseband, the periodic rectangular wave can be expanded into Fourier series, in which only the first harmonic term is used for the convenience in the following calculation. As a result, the mesh stiffness K can be expressed as follows:

$$K(t) = K_m + K_a \sin(\omega t + \varphi_0) \tag{7}$$

Where, K_m is the average mesh stiffness, K_a is the stiffness fluctuation amplitude, λ is the stiffness fluctuation coefficient which is equal to K_m / K_a, ω is the mesh frequency, and φ_0 is the initial phase. At the same time, the mesh damping of the gear set can be expressed as:

$$C = 2\zeta\sqrt{K_m / (1/M_1 + M_2)} \tag{8}$$

Where, ζ is the damping ratio, M is the equivalent mass which is equal to J / r_b^2, and the subscripts 1 and 2 represent the master gear and driven gear, respectively. Because of the compact arrangement of the gear reducer and the thicker structure of transmission shaft, the inertia can be distributed to the adjacent gears according to the law of the same center of mass, neglecting the effect on deformation. Therefore, the mesh damping of the parts can be expressed as follows:

$$C_{spi} = 2\xi_{spi}\sqrt{\frac{k_{spi} J_s J_{pi}}{J_s r_{bpi}^2 + J_{pi} r_{bs}^2}} \tag{9}$$

As the carrier is fixed, the inertia of the carrier tends to infinity, at the same time the mesh damping between the planet gear and the carrier can be expressed as follows:

$$C_{rpi} = 2\xi_{rpi}\sqrt{\frac{k_{rpi} J_{pi}}{r_{bpi}^2}} \tag{10}$$

Assuming that the composite mesh error is the sin function which is changed with the mesh cycle of the planetary gear train, the dynamic mash error of the parts can be expressed as follows:

$$\begin{cases} e_{spi}(t) = E_{spi} \sin(\omega t + \phi_{spi}) \\ e_{rpi}(t) = E_{rpi} \sin(\omega t + \phi_{rpi}) \end{cases} \tag{11}$$

Where, E is the composite frequency error, ω is the mesh frequency of the planetary gear train. As the dynamic model of the planetary gear is established along the meshing line, the backlash is measured in meshing line. Taking the backlash as a symmetric function according to the description in the paper [13], then the nonlinear backlash can be expressed as follows:

$$f(x,b)=\begin{cases} x-b & (x>b) \\ 0 & (-b\le x\le b) \\ x+b & (x<-b) \end{cases} \tag{12}$$

Because of the strong nonlinearity of the backlash and the repeated call of the backlash, it will make troubles in computational process, causing a sharp divergence of solving speed. To solve it, a hyperbolic tangent function tanh (Figure 4) is used to approximate the traditional piecewise linear function, the specific expression is shown as follows:

$$\begin{aligned} f(x,b)=x+\frac{1}{2}[\tanh(\sigma_\infty\cdot(x-b))-\tanh(\sigma_\infty\cdot(x+b))] \\ -\frac{b}{2}[\tanh(\sigma_\infty\cdot(x-b))+\tanh(\sigma_\infty\cdot(x+b))] \end{aligned} \tag{13}$$

Where, σ_∞ is the amplification coefficient of backlash. According to Figure 5, there will be a good approximation to equation (12) when σ_∞ is amplified to 1000.

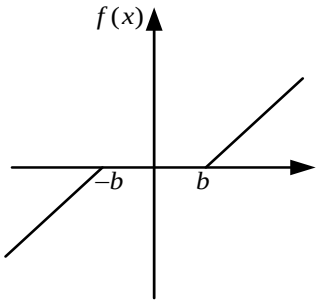

Figure 4. Nonlinear Expression of Backlash

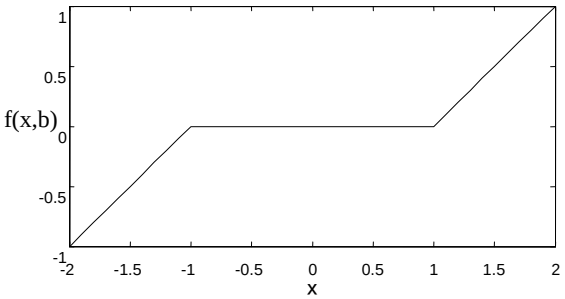

Figure 5. Fitting Result of Backlash ($\sigma_\infty=1000b$)

Whereas the approximation function is composed of linear part and nonlinear part, the nonlinear part can be moved to the right side as a pseudo excitation. In conclusion, Equations (1)-(3) can be rewritten in the following matrix form as:

$$\begin{cases} M\ddot{\theta}+C\dot{\theta}+K\cdot f(\theta)=F(t,\theta,\dot{\theta}) \\ \theta=[\theta_s,\theta_{pi},\theta_c]^T \end{cases} \tag{14}$$

Where, M is constant diagonal inertia matrix, F is the pseudo excitation torque including motor torque, load torque and transmission error. So far, the dynamic model of joint with planetary gear reducer is established.

3. Solution of Dynamic Model

3.1. The Dimensionless Processing to Joint Dynamic Model

Under the international standard units, the stiffness coefficient is usually fluctuating between 10^7 □ 10^8, whereas the damping ratio is fluctuating between 10^{-4} □ 10^{-1}. Owing to the large difference in order of magnitudes, it will bring great difficulties in the process of calculation during the numerical analysis. Therefore, a set of new coordinate variables X are defined, by which means not only can solve the problem, but also eliminate the rigid body displacement.

$$X = \{X_{sp1}, X_{sp2}, \cdots X_{spn}, X_{sc}\}^T \tag{15}$$

Wherein,

$$X_{sp1} = \frac{\theta_s r_{bs} - \theta_{pi} r_{bpi} - \theta_c r_c \cos\alpha - e_{spi}(t)}{b_c} \tag{16}$$

$$X_{sc} = \frac{\theta_s r_{bs} - 2\theta_c r_c \cos\alpha}{b_c} \tag{17}$$

In addition, dimensionless parameters can be obtained by a characteristic length b_c and frequency ω_n, where the expression ω_n is shown in equation (18). At the same time, the dimensionless time can be defined as τ which is equal to ω_n multiple the time t.

$$\omega_n = \sqrt{K_m(1/M_s + 1/M_{pi})} \tag{18}$$

According to equation (14)-(18), the dynamic model can be rewritten to the following differential equations:

$$\begin{cases} \ddot{X}_{spi} + \frac{1}{\omega_n^2}(\frac{1}{M_s} + \frac{1}{M_c})\sum_{i=1}^{n} K_{spi}(\tau) f(X_{spi}, \bar{b}_{spi}) + \frac{1}{\omega_n^2 M_{pi}} K_{spi}(\tau) f(X_{spi}, \bar{b}_{spi}) + \frac{1}{\omega_n}(\frac{1}{M_s} + \frac{1}{M_c})\sum_{i=1}^{n} C_{spi}\dot{X}_{spi} \\ -\frac{1}{\omega_n^2 M_{pi}} K_{rpi}(\tau) f(X_{sc} - X_{spi} - \bar{e}_{spi}(\tau) - \bar{e}_{rpi}(\tau), \bar{b}_{rpi}) + \frac{1}{\omega_n^2 M_c}\sum_{i=1}^{n} K_{rpi}(\tau) f(X_{sc} - X_{spi} - \bar{e}_{spi}(\tau) - \bar{e}_{rpi}(\tau), \bar{b}_{rpi}) \\ -\frac{1}{\omega_n M_{pi}} C_{rpi}(\dot{X}_{sc} - \dot{X}_{spi} - \dot{\bar{e}}_{spi}(\tau) - \dot{\bar{e}}_{rpi}(\tau)) + \frac{1}{\omega_n M_{pi}} C_{spi}\dot{X}_{spi} + \frac{1}{\omega_n M_c}\sum_{i=1}^{n} C_{rpi}(\dot{X}_{sc} - \dot{X}_{spi} - \dot{\bar{e}}_{spi}(\tau) - \dot{\bar{e}}_{rpi}(\tau)) \\ = \frac{T_D}{M_s r_{bs}\omega_n^2 b_c} + \frac{T_L}{M_c r_c \omega_n^2 b_c \cos\alpha} - \ddot{\bar{e}}_{spi}(\tau) \\ \ddot{X}_{sc} + \frac{1}{\omega_n^2}(\frac{1}{M_s} + \frac{2}{M_c})\sum_{i=1}^{n} K_{spi}(\tau) f(X_{spi}, \bar{b}_{spi}) + \frac{2}{\omega_n^2 M_c} K_{rpi}(\tau) f(X_{sc} - X_{spi} - \bar{e}_{spi}(\tau) - \bar{e}_{rpi}(\tau), \bar{b}_{rpi}) + \\ \frac{1}{\omega_n}(\frac{1}{M_s} + \frac{2}{M_c})\sum_{i=1}^{n} C_{spi}\dot{X}_{spi} + \frac{2}{\omega_n M_c}\sum_{i=1}^{n} C_{rpi}(\dot{X}_{sc} - \dot{X}_{spi} - \dot{\bar{e}}_{spi}(\tau) - \dot{\bar{e}}_{rpi}(\tau)) = \frac{T_D}{M_s r_{bs}\omega_n^2 b_c} + \frac{2T_L}{M_c r_c \omega_n^2 b_c \cos\alpha} \end{cases} \tag{19}$$

Where,

$M_c = \frac{J_c + \sum_{i=1}^{n} m_{pi} r_c^2}{r_c^2 \cos^2\alpha}$, $\bar{e}_{spi}(\tau) = \frac{E_{spi}}{b_c}\sin(\Omega\tau + \phi_{spi})$, $\bar{e}_{rpi}(\tau) = \frac{E_{rpi}}{b_c}\sin(\Omega\tau + \phi_{rpi})$

$\bar{b}_{spi}(\tau) = b_{spi}/b_c$, $\bar{b}_{rpi}(\tau) = b_{rpi}/b_c$, $\Omega = \omega/\omega_n$.

Through the above dimensionless processing, the degrees of freedom of the original second-order differential equations have been converted from n+2 into n+1. It is concluded that an appropriate coordinate transformation to the system can not only reduce the number of unknown variables in the equation set, but also lower the dimensionality of equations.

3.2. Numerical Solution of Dynamic Model

Generally speaking, there are two kinds of calculation methods solving the differential equations, including analytical method and numerical integration [14]. Among them, because of the restrictions of the excitation assumption and response form, the process of solving the differential equations in analytical method is very cumbersome, which even artificially loses the super harmonic response, the second harmonic response and chaos component. Under such circumstance, the numerical integral method is used to solve the problem through calculating the equations under Hamiltonian system, where the second-order differential equation can be converted into first-order differential equation. Through the processing of reduced order, the amount of calculation is reduced. In order to replace the original equations with first-order differential systems, a set of new coordinate variables $v = (v_1, v_2, \cdots v_{2n})^T$ is defined which can be written as follows:

$$\begin{cases} \dot{v} = Hv + f \\ v = (X^T, Y^T)^T \end{cases} \tag{20}$$

Where

$$Y = M\dot{X} + 1/2CX, \quad H = \begin{bmatrix} -1/2M^{-1}C & M^{-1} \\ 1/4CM^{-1}C - K & -1/2CM^{-1} \end{bmatrix}, \quad f = \begin{pmatrix} 0 \\ F \end{pmatrix}.$$

Seen from the equation (20), the solution to vector x has been changed into vector v which means that the solving of second-order differential equation has been convert into the first-order differential equation, where H is the linear item and f is the nonlinear part. Through the above processing, the solving difficulty of nonlinear equations is reduced, at the same time the precise integration algorithm [15] can be used to handle with first-order differential equation. Due to the simple principle of precise integration algorithm, the steady-state response results can be obtained by means of few codes with high run speed.

4. Numerical Simulation

In this section, the differential equations will be solved numerically by precise integration algorithm (integration step is 1ms). The main parameters of the planetary gear transmission joint shown in Figure 1 (the planetary has 3 planet gears) are given in Table 1. In this study, the value of average mesh stiffness K_m is 10^8, and the initial phase angle of frequency error is assumed to be 0.

Table 1. The Main Parameters of Planetary Gear Train

	Sun gear	Planetary gear	Carrier	Ring gear
Number of teeth	27	35	—	99
Module	—	3	—	—
Pitch radius	40.5	52.5	92.5	148.5
Mass	0.40	0.66	2.35	5.43
Pressure angle	—	24.6°	—	—
Inertia	0.39	0.61	3.00	6.29

The phase diagram can be used to analyze the dynamic characteristics due to the core is to analyze the influence of backlash to gear periodic solutions. Assuming that the backlash values are both $2b$ between the meshing of sun-planets and planet-ring gear, the steady-state response can be calculated under different backlash values, which is characterized using the dimensionless displacement X. Owing to the similar variation between X_{sc} and X_{spi}, only the result of respond X_{spi} is given as follows:

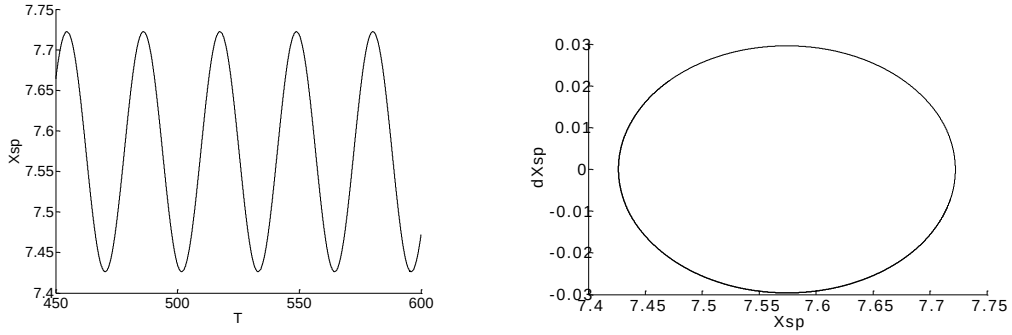

(a) Time (b) Phase diagram

Figure 5. Dynamic Response when $b = 0\mu m$

Where, T is the dimensionless time. Seen from Figure 5, the steady-state response of displacement X_{sp} is periodic motion and the graph is a closed ellipse when backlash is zero.

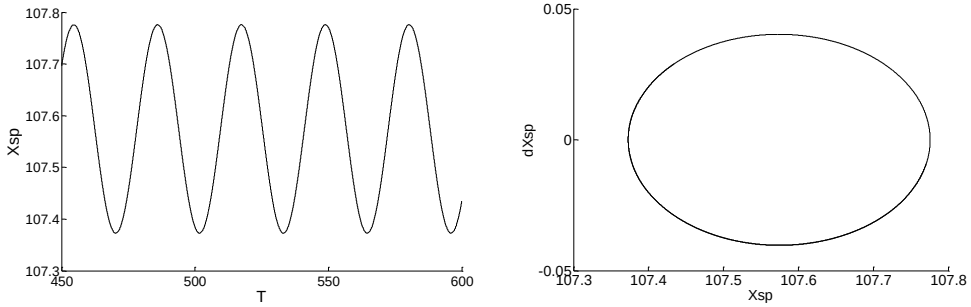

(a) Time (b) Phase diagram

Figure 6. Dynamic Response when $b = 10\mu m$

It is obvious from the comparison between Figure 5 and Figure 6 that the variations are similar, so the existence of backlash has less effect on dynamic response of the system when b is equal to $10\mu m$.

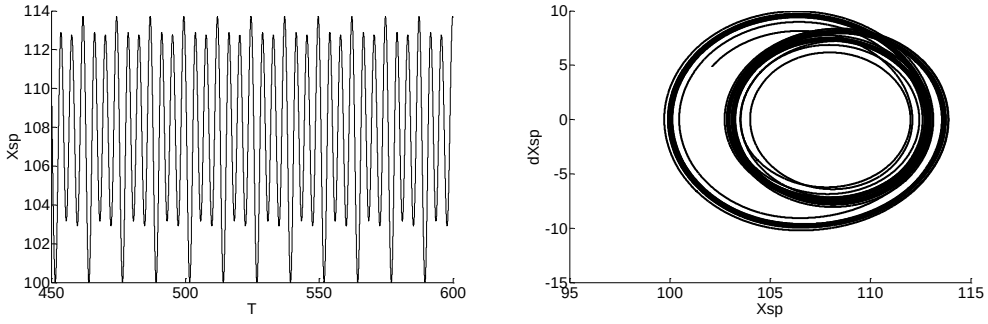

(a) Time (b) Phase diagram

Figure 7. Dynamic Response when $b = 60\mu m$

Seen from Figure 7, the steady-state response of system is harmonic respond when the backlash is $60\mu m$. So, the dynamic respond will be changed with the increasing of backlash.

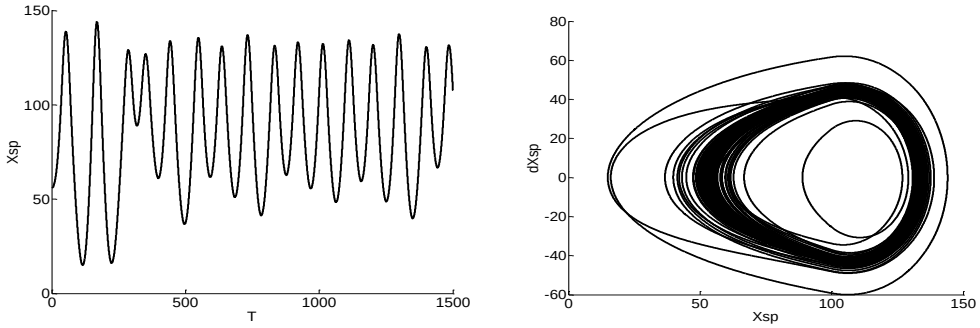

(a) Time (b) Phase diagram

Figure 8. Dynamic Response when $b = 120\mu m$

Seen from Figure 8, the steady-state response of system is Chaos respond when the backlash is $120\mu m$.

It is concluded that the backlash within a certain range has less effect on periodic solutions of the planetary gear transmission train, but with the enlargement of backlash, the response quickly changed from single frequency response to the chaos, which will bring in strong meshing shock according to Figure 5-8. Therefore, it is necessary to consider the existence of backlash in the process of modeling of planetary gear reducer transmission.

5. Conclusion

In order to analyze the influence on gear transmission joint with backlash, a comprehensive dynamic model of planetary gear transmission joints is established by the lumped parameter method with the consideration of time-varying mesh stiffness, mesh damping, gear backlash and gear mesh error. In addition, the differential equations of motion are established by Newton-Euler method in this study. On the basis of an approximate treatment to the nonlinear backlash according to the characteristic of function tanh and a dimensionless processing to the dynamic model, the differential equations are solved analytically using the precise integration algorithm under Hamiltonian system. In the above process, the appropriate coordinate transformation to system can reduce the dimensionality of equations, while the solving of differential equations under Hamiltonian system can lower the order. Ultimately, the steady-state response results can be obtained, where the simulation results indicate that:

(1) The backlash within a certain range has little effect on periodic solutions of planetary gear transmission train, and the dynamic response of system is the same as a linear system.
(2) With the increasing enlargement of backlash, the response quickly turns from single frequency response to the chaos, which will bring in strong meshing shock. So the research on compensating control strategy of the planet gear with backlash is necessary.

Acknowledgements

This work is supported by the National Key Basic Research Program of China (2013CB733000), and the National Natural Science Foundation of China (61175080).

References

[1]. Pan and D. Y. Yu, Journal of Astronautics, vol. 31, no. 11, **(2010)**, pp. 2448-2455.
[2]. A. Tasora, E. Prati and M. Silvestri, "A Compliant Measuring System for Revolute Joints with Clearance", Proceedings of the 2006 International Conference on Tribology, **(2006)** September 20-22; Parma, Italy.

[3]. Q. Tian, Y. Q. Zhang and L. P. Computers and Structures, vol. 87, no. 11, **(2009)**, pp. 913-929.
[4]. S. Erkaya and I. Uzmay, Mechanism and Machine Theory, vol. 44, no. 1, **(2009)**, pp. 222-234.
[5]. Z. M. Sun, L. H. Ji and Y. W. Shen, Journal of Tsinghua University (Science and Technology), vol. 43, no.5, **(2003)**, pp. 636-639.
[6]. H. Moradi and H. Salarieh, Mechanism and Machine Theory, vol. 51, no. 5, **(2012)**, pp. 14-31.
[7]. Q. Huang, Y. Wang and Z. Huo, Mathematical Problems in Engineering, vol. 2013, **(2013)**, pp. 1-12.
[8]. Y. Chen, X. Wu and J. Jin, International Conference on Intelligent Human-Machine Systems and Cybernetics, vol. 1, **(2009)**, pp.21-24.
[9]. Y. Guo and R. G. Parker, European Journal of Mechanics-A/Solids, vol. 29, no. 6, **(2010)**, pp. 1022-1033.
[10]. T. Sun and H. Y. Hu, Mechanism and Machine Theory, vol. 38, no. 12, **(2003)**, pp. 1371-1390.
[11]. J. W. Lu and H. Chen, Journal of Mechanical Engineering, vol. 49, no. 15, **(2013)**, pp. 15-21.
[12]. Q. Q. Wei, Y. B. Wang and Z. Q. Liu, Chinese Space Science and Technology, vol. 10, no. 5, **(2013)**, pp. 76-81.
[13]. J. Vörös, Automatica, vol. 46, no. 2, **(2013)**, pp. 369-374.
[14]. P. Flores, Mechanism and machine theory, vol. 44, no. 6, **(2009)**, pp. 1211-1222.
[15]. C. H. Qiu and H. X. Lu, Chinese Journal of Computational Mechanics, vol. 17, no. 2, **(2000)**, pp. 127-132.

Authors

Shiwen He is currently a graduate student in Pattern Recognition and Intelligent Control at Beijing University of Posts and Telecommunications and has an interest in robotics and robust control, in particular the compensation control with gear backlash.

Qingxuan Jia is a Professor of Automation at Beijing University of Posts and Telecommunications (BUPT). He received his B. S. degree in Shandong University of Technology in 1982, and received his M.S. and Ph.D. degrees in Beijing University of Aeronautics and Astronautics in 1991 and 2005, respectively. His research interests are the basic theory and key technology of frontier disciplines in advanced robotics, including space robot, mobile robot and so on.

